

Electronic Structure of Iron Chlorins: Characterization of Bis(L-valine methyl ester)(*meso*-tetraphenylchlorin)iron(III)triflate and Bis(L-valine methyl ester)(*meso*-tetraphenylchlorin)iron(II)

G rard Simonneau,^{*,†} Marwan Kobeissi,[†] and Loic Toupet[‡]

Laboratoire de Chimie Organom tallique et Biologique, UMR CNRS 6509,
and Groupe Mati re Condens e et Mat riaux, UMR CNRS 6626,
Universit  de Rennes 1, Campus de Beaulieu, 35042 Rennes Cedex, France

Received September 17, 2002

The synthesis and characterization of the two iron chlorin complexes [Fe^{III}(TPC)(NH₂CH(CO₂CH₃)(CH(CH₃)₂))₂]-CF₃SO₃ (**1**) and Fe^{II}(TPC)(NH₂CH(CO₂CH₃)(CH(CH₃)₂))₂ (**2**) are reported. The crystal structure of complex **1** has been determined. The X-ray structure shows that the porphyrinate rings are weakly distorted. The metal–nitrogen distances to the reduced pyrrole N(4), 2.034(4)  , and to the pyrrole trans to it N(2), 2.012(4)  , are longer than the distances to the two remaining nitrogens [N(1), 1.996(4)  , and N(3), 1.984(4)  ], leading to a core–hole expansion of the macrocycle due to the reduced pyrrole. The ¹H NMR isotropic shifts at 20  C of the different pyrrole protons of **1** varied from –0.8 to –48.3 ppm according to bis-ligated complexes of low-spin ferric chlorins. The EPR spectrum of [Fe(TPC)(NH₂CH(CO₂CH₃)(CH(CH₃)₂))₂CF₃SO₃ (**1**) in solution is rhombic and gives the principal *g* values *g*₁ = 2.70, *g*₂ = 2.33, and *g*₃ = 1.61 ($\Sigma g^2 = 15.3$). These spectroscopic observations are indicative of a metal-based electron in the d_{xy} orbital for the [Fe(TPC)(NH₂CH(CO₂CH₃)(CH(CH₃)₂))₂CF₃SO₃ (**1**) complex with a (d_{xy})²(d_{xz}d_{yz})³ ground state at any temperature. The X-ray structure of the ferrous complex **2** also shows that the porphyrinate rings are weakly distorted. The metal–nitrogen distances to the reduced pyrrole N(4), 1.991(5)  , and to the pyrrole trans to it N(2), 2.005(6)  , are slightly different from the distances to the two remaining nitrogens [N(1), 1.988(5)  , and N(3), 2.015(5)  ], leading to a core–hole expansion of the macrocycle due to the reduced pyrrole.

Introduction

Nature utilizes iron chlorins as the active sites of numerous heme enzymes such as heme *d* found in a terminal oxidase complex from *Escherichia coli*.^{1–4} Heme *d* has also been found in catalases, such as hydroperoxidase II, from *Escherichia coli*.⁵ In contrast to cytochrome *bd* oxidase, the crystal structure of catalase HP II from *Escherichia coli* (*E.*

coli), has been determined to contain a heme *d* prosthetic group with a *cis*-hydroxychlorin γ -spirolactone⁶ and a tyrosine as the proximal ligand.⁷ A heme *d* prosthetic group with the same configuration has also been found in the crystal structure of *Penicillium vitale* catalase.⁸ Evidence favoring coordination of a tyrosinate proximal ligand to the chlorin iron of *E. coli* Hp II catalase was previously presented by Dawson et al.⁹ In sulfmyoglobin, a nonfunctional form of myoglobin, the porphyrin macrocycle has been reduced to a chlorin by the addition of a sulfur atom to a pyrrole ring.¹⁰

* To whom correspondence should be addressed. E-mail: simonnea@univ-rennes1.fr.

† UMR CNRS 6509.

‡ UMR CNRS 6626.

- (1) Sun, J.; Khalow, M. A.; Kaysser, T. M.; Osborne, J. P.; Hill, J. J.; Rohlfs, R. J.; Hille, R.; Gennis, R. B.; Loehr, T. M. *Biochemistry* **1996**, *35*, 2403–2412.
- (2) Sun, J.; Osborne, J. P.; Khalow, M. A.; Kaysser, T. M.; Gennis, R. B.; Loehr, T. M. *Biochemistry* **1995**, *34*, 12144–12151.
- (3) J nemann, S. *Biochim. Biophys. Acta* **1997**, *1321*, 107–127.
- (4) Borisov, V. B.; Liebl, U.; Rappaport, F.; Martin, J. L.; Zhang, J.; Gennis, R. B.; Konstantinov, A. A.; Vos, M. H. *Biochemistry* **2002**, *41*, 1654–1662.
- (5) Chiu, J. T.; Loewen, P. C.; Switala, J. G.; R. B.; Timkovich, R. J. *Am. Chem. Soc.* **1989**, *111*, 7046–7050.

- (6) Andersson, L. A.; Sotiriou, C.; Chang, C. K.; Loehr, T. M. *J. Am. Chem. Soc.* **1987**, *109*, 258–264.

- (7) Bravo, J.; Verdaguer, N.; Tormo, J.; Betzel, C.; Switala, J.; Loewen, P. C.; Fita, I. *Structure* **1995**, *3*, 491–502.
- (8) Murshudov, G. N.; Grebenko, A. I.; Barynin, V.; Dauter, Z.; Wilson, K. S.; Vainshtein, B. K.; Melik-Adamyam, W.; Bravo, J.; Ferran, J. M.; Ferrer, J. C.; Switala, J.; Loewen, P. C.; Fita, I. *J. Biol. Chem.* **1996**, *271*, 8863–8868.
- (9) Dawson, J. H.; Bracete, A. M.; Huff, A. M.; Kadkhodayan, S.; Zeitler, C. M.; Sono, M.; Chang, C. K.; Loewen, P. C. *FEBS Lett.* **1991**, *295*, 123–126.

Iron chlorins are porphyrin-derived iron-containing prosthetic groups in which one of the peripheral double bonds of the porphyrin ring has been reduced to yield a dihydroporphyrin. Although some investigations of the NMR and EPR spectra of low-spin iron(III) complexes of reduced porphyrins have been investigated by us^{11,12} and others,^{10,13–22} the nature of the electronic ground state is not always clear, and more information is needed on these systems. Magnetic circular dichroism spectroscopy has also been shown to be of great utility in the identification of proximal and distal axial ligands in chlorin-containing proteins.^{23,24} However, only a limited number of iron chlorin complexes such as high-spin ferrous,^{25,26} high-spin ferric,^{21,27} (μ -oxo) bis-[(tetraphenylchlorin)iron(III)],²⁸ and low-spin ferric tetraphenylporphyrin¹¹ species have been investigated with X-ray crystallography.

We now report two X-ray structures and ¹H NMR analyses of the bis(L-valine methyl ester) adduct of ferric and ferrous tetraphenylporphyrins as low-spin complexes. The purpose of this study is to extend the coverage of iron chlorin models with possible physiological nitrogenous ligands such as amino acids. It should be emphasized that such a group was recently found as the axial ligand in cytochrome *f*.^{29–31} Cytochrome *f* is one of the four redox centers in the

cytochrome *b₆f* complex of the thylakoid membrane in oxygenic photosynthetic organisms. Cytochrome *f* is also the electron donor to the Cu-containing protein plastocyanin in some eukariotic algae and cyanobacteria, when grown in a Cu-deficient environment. The protein consists predominantly of β -sheets and has a unique ligation of the heme by the α -amino N of the N-terminal residue. The structures of two truncated forms of the protein have been reported, one from turnip^{29,30} and the other one from *Chlamydomonas reinhardtii*.^{31,32} Some examples of iron porphyrin complexes bearing amino esters³³ (or amino acids)³⁴ have been reported, but no X-ray structural data are yet available.

Experimental Section

General Procedures and Materials. All reactions were performed under argon atmosphere using standard Schlenk techniques. Solvents were distilled from phosphorus pentoxide (dichloromethane) and sodium (pentane). Fe(TPC)CF₃SO₃ was prepared as previously reported.¹² Amino esters are commercially available as their hydrochloride salts. The salts were dissolved in NaOH solution (2 N). The solutions were stirred at room temperature for 15 min. The amino esters were extracted with ether and dried under vacuum.

Physical Measurements. UV–visible spectra were recorded on a Uvikon 941 spectrophotometer in dichloromethane. ¹H NMR spectra were recorded in CD₂Cl₂ on a Bruker 200 DPX spectrometer (200 MHz), and chemical shifts are referenced to internal TMS. EPR spectra were recorded in CH₂Cl₂ on a Bruker EMX 8/2,7 spectrometer operating at X-band frequencies. Samples were cooled to 4.2 K in a stream of helium gas in frozen CH₂Cl₂, the temperature of which was controlled by an Oxford Instruments ESR 900 cryostat. Mass spectrometry was performed by the Centre Régional de Mesures Physiques de l'Ouest (CRMPO), Rennes, France

Abbreviations used: TPC = 7,8-dihydro-5,10,15,20-tetraphenylporphyrin dianion (tetraphenylchlorin), TPP = 5,10,15,20-tetraphenylporphyrin.

Syntheses. [Fe(TPC)(NH₂CH(CO₂CH₃)(CH(CH₃)₂))₂]CF₃SO₃ (**1**). To a solution of 0.05 g (0.06 mmol) of Fe(TPC)CF₃SO₃ in 2 mL of dichloromethane was added 2.5 equiv (22 μ L, 0.15 mmol) of L-valine methyl ester by a syringe under stirring at room temperature. After being stirred for 15 min, the solution became green. Then, 2 mL of toluene and 6 mL of hexane were added, and the solution was set aside overnight for crystallization at 0 °C. Purple crystals of [Fe(TPC)(NH₂CH(CO₂CH₃)(CH(CH₃)₂))₂]CF₃SO₃ (**1**) were collected by filtration and washed with hexane. The yield was 0.054 g (82%). UV–vis (CH₂Cl₂): $\lambda_{\text{max}}/\text{nm}$ 413 (ϵ 119 dm³ mmol⁻¹ cm⁻¹), 548 (ϵ 10.6), 600 (ϵ 12.8), 638 (ϵ 15.5). ¹H NMR δ_{ppm} (CD₂Cl₂): chlorin -0.8 (s, 2H, pyrrole), -16.4 (s, 2H, pyrrole), -48.3 (s, 2H, pyrrole), 6.1 (s, 4H, ortho), 6.4 (s, 4H, ortho'), 6.82 (s, 4H, meta), 6.84 (s, 4H, meta'), 7.12 (t, 2H, para), 6.8 (t, 2H, para'), 58 (s, 2H, pyrroline), 63 (s, 2H, pyrroline); ligand 175.6 (b, 4H, NH₂), -4.2 (b, 2H, CHa), 8.03 (b, 2H, CHb), 4.66 (b, 6H, CH₃), 2.94 (b, 6H, CH₃), 3.53 (b, 6H, CO₂CH₃). MS (FAB) Found: *m/z* 670.38. Calcd for C₅₆H₅₆N₆O₄Fe: [M - 2(NH₂CH(CO₂CH₃)(CH(CH₃)₂))] +, 670.7.

- (10) Chatfield, M. J.; La Mar, G. N.; Parker, W. O.; Smith, K. M.; Leung, H. K.; Morris, I. M. *J. Am. Chem. Soc.* **1988**, *110*, 6352–6358.
- (11) Kobeissi, M.; Toupet, L.; Simonneaux, G. *Inorg. Chem.* **2001**, *40*, 4494–4499.
- (12) Simonneaux, G.; Kobeissi, M. *J. Chem. Soc., Dalton Trans.* **2001**, 1587–1592.
- (13) Stolzenberg, A. M.; Strauss, S. H.; Holm, R. H. *J. Am. Chem. Soc.* **1981**, *103*, 4763–4778.
- (14) Muhoberac, B. B. *Arch. Biochem. Biophys.* **1984**, *233*, 682–697.
- (15) Morishima, I.; Fujii, H.; Shiro, Y. *J. Am. Chem. Soc.* **1986**, *108*, 3858–3860.
- (16) Licoccia, S.; Chatfield, M. J.; La Mar, G.; Smith, K. M.; Mansfield, K. E.; Anderson, R. R. *J. Am. Chem. Soc.* **1989**, *111*, 6087–6093.
- (17) Keating, K. A.; de Ropp, J. S.; La Mar, G. N.; Balch, A. L.; Shiao, F. Y. *Inorg. Chem.* **1991**, *30*, 3258–3263.
- (18) Ozawa, S.; Watanabe, Y.; Morishima, I. *Inorg. Chem.* **1992**, *31*, 4042–4043.
- (19) Ozawa, S.; Watanabe, Y.; Morishima, I. *J. Am. Chem. Soc.* **1994**, *116*, 5832–5838.
- (20) Jayaraj, K.; Gold, A.; Austin, R. N.; Mandon, D.; Weiss, R.; Terner, J.; Bill, E.; Muther, M.; Trautwein, A. X. *J. Am. Chem. Soc.* **1995**, *117*, 9079–9080.
- (21) Wojaczynski, J.; Latos-Grazynski, L.; Glowiak, T. *Inorg. Chem.* **1997**, *36*, 6299–6306.
- (22) Astashkin, A. V.; Raitsimring, A. M.; Walker, F. A. *J. Am. Chem. Soc.* **2001**, *123*, 1905–1913.
- (23) Huff, A. M.; Chang, C. K.; Cooper, D. K.; Smith, K. M.; Dawson, J. H. *Inorg. Chem.* **1993**, *32*, 1460–1466.
- (24) Bracete, A. M.; Kadkhodayan, S.; Sono, M.; Huff, A. M.; Zhuang, C.; Cooper, D. K.; Smith, K. M.; Chang, C. K.; Dawson, J. H. *Inorg. Chem.* **1994**, *33*, 5042–5049.
- (25) Strauss, S. H.; Silver, M. E.; Ibers, J. A. *J. Am. Chem. Soc.* **1983**, *105*, 4108–4109.
- (26) Strauss, S. H.; Silver, M. E.; Long, K. M.; Thompson, R. G.; Hudgens, R. A.; Spartalian, K.; Ibers, J. A. *J. Am. Chem. Soc.* **1985**, *107*, 4207–4215.
- (27) Jayaraj, K.; Gold, A.; Austin, R. N.; Ball, L. M.; Terner, J.; Mandon, D.; Weiss, R.; De Cian, A.; Bill, E.; Muther, M.; Schünemann, V.; Trautwein, A. X. *Inorg. Chem.* **1997**, *36*, 4555.
- (28) Strauss, S. H.; Pawlik, M. J.; Skowrya, J.; Kennedy, J. R.; Anderson, O. P.; Spartalian, K.; Dye, J. L. *Inorg. Chem.* **1987**, *26*, 724–730.
- (29) Martinez, S. E.; Huang, D.; Szecepaniak, A.; Cramer, W. A.; Smith, J. L. *Structure* **1994**, *2*, 95–105.
- (30) Martinez, S. E.; Huang, D.; Ponomarev, M.; Cramer, W. A.; Smith, J. L. *Protein Sci.* **1996**, *5*, 1081–1092.
- (31) Chi, Y. I.; Huang, L. S.; Zhang, Z.; Fernandez-Velasco, J. G.; Berry, E. A. *Biochemistry* **2000**, *39*, 7689–7701.

- (32) Sainz, G.; Carrell, C. J.; Ponomarev, M. V.; Soriano, G. M.; Cramer, W. A.; Smith, J. L. *Biochemistry* **2000**, *39*, 9164–9173.
- (33) Morice, C.; Le Maux, P.; Simonneaux, G. *Inorg. Chem.* **1998**, *37*, 6100–6103.
- (34) Gilbert, B. C.; Lindsay Smith, J. R.; Parsons, A. F.; Setchell, P. K. *J. Chem. Soc., Perkin Trans. 2* **1997**, 1065–1073.

Table 1. Crystallographic Data for [Fe(TPC)(NH₂CH(CO₂CH₃)(CH(CH₃)₂))₂]CF₃SO₃ (**1**) and [Fe(TPC)(NH₂CH(CO₂CH₃)(CH(CH₃)₂))₂] (**2**)

	1 (CH ₂ Cl ₂)	2
empirical formula	C ₅₇ H ₅₆ FeF ₃ N ₆ O ₇ S	2(C ₅₆ H ₅₆ FeN ₆ O ₄)
FW	1164.9	1865.84
crystal system	triclinic	monoclinic
space group	P1	P21
<i>a</i> , Å	11.0760(4)	11.5024(2)
<i>b</i> , Å	11.3880(4)	18.4184(3)
<i>c</i> , Å	12.7130(7)	23.6580(6)
α , deg	105.190(2)	—
β , deg	96.510(2)	102.898(6)
γ , deg	113.190(2)	—
<i>V</i> , Å ³	1379.4(1)	4885.6(2)
<i>Z</i>	1	4
ρ_{calcd} , g cm ⁻³	1.402	1.268
μ , cm ⁻¹	0.48	3.62
<i>T</i> , K	110	293
<i>R</i> _w	0.134	0.174
final <i>R</i>	0.053	0.059

Fe(TPC)(NH₂CH(CO₂CH₃)(CH(CH₃)₂))₂] (2**).** A solution of Fe(TPC)Cl (0.1 g, 0.14 mmol) in dichloromethane was reduced under argon by Zn–Hg amalgam. The solution was then filtered, and 8 equiv of valine methyl ester was added by a syringe to the in situ Fe(TPC) species. Hexane (30 cm³) was added gradually, and the solution was set aside overnight for crystallization at 0 °C. Fine crystals of Fe(TPC)[(NH₂CH(CO₂CH₃)(CH(CH₃)₂))₂] were collected by filtration. The yield was 0.1 g (75%). UV–vis (CH₂-Cl₂): λ_{max} /nm 422 (ϵ 100 dm³ mmol⁻¹ cm⁻¹), 555 (ϵ 8.6), 609 (ϵ 17), 645 (ϵ 5.5).

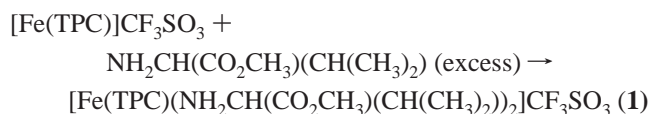
X-ray Structure Determinations. Both X-ray studies were carried out on a Nonius Kappa CCD with graphite-monochromatized Mo K α radiation. The cell parameters were obtained with Denzo and Scalepack³⁵ with 10 frames (Φ rotation = 1° per frame). Crystallographic data are listed in Table 1. Crystals of the compounds were obtained as reported in the Results and Discussion section. Atomic scattering factors were from *International Tables for X-ray Crystallography*.³⁶ Ortep views were realized with PLATON98.³⁷ All calculations were performed on a Pentium NT Server computer

Single-Crystal Structure Determination on [Fe(TPC)(NH₂CH(CO₂CH₃)(CH(CH₃)₂))₂]CF₃SO₃ (1**).** The data collection ($2\theta_{\text{max}} = 60^\circ$; 189 frames via 2.0° ω rotation and 40 s per frame; range *h,k,l* *h* = 0–14, *k* = –14 to 14, *l* = –16 to 16) gave 18 987 integrated reflections. The data reduction led to 6250 independent reflections, of which 5096 reflections satisfied $I > 2.0\sigma(I)$. The structure was solved with SIR-97, which reveals all of the non-hydrogen atoms of the compound and the solvent.³⁸ After anisotropic refinement, many hydrogen atoms were found by Fourier difference. The whole structure was refined by the full-matrix least-squares techniques with SHELXL97,³⁹ including use of $|F^2|$; *x*, *y*, *z*, β_{ij} for Fe, N, Cl, S, O, and C atoms and riding mode for H atoms; 708 variables and 5096 observations with $I > 2.0\sigma(I)$; calc $w = 1/[\sigma^2(F_o)^2 + (0.096P)^2 + 0.198P]$, where $P = (F_o^2 + 2F_c^2)/3$, with the resulting $R = 0.053$, $R_w = 0.134$, and $S_w = 1.035$ (residual $\Delta\rho < 0.72$ eÅ⁻³).

Single-Crystal Structure Determination on Fe(TPC)(NH₂CH(CO₂CH₃)(CH(CH₃)₂))₂] (2**).** The data collection ($2\theta_{\text{max}} = 60^\circ$; 218 frames via 1.0° ω rotation and 13 s per frame; range *h,k,l* *h* = 0–14, *k* = 0 to 23, *l* = –29 to 30) gave 42 777 reflections. The data reduction led to 11 439 independent reflections, of which 6489 reflections satisfied $I > 2.0\sigma(I)$. The structure was solved with SIR-97, which reveals the non-hydrogen atoms of the compound.³⁸ The two resulting complexes are designated **2A** and **2B**. After anisotropic refinement, many hydrogen atoms were found by Fourier difference. The whole structure was refined by the full-matrix least-squares techniques with SHELXL97,³⁹ including use of $|F^2|$; *x*, *y*, *z*, β_{ij} for Fe, N, O, and C atoms and riding mode for H atoms; 1208 variables and 6489 observations with $I > 2.0\sigma(I)$; calc $w = 1/[\sigma^2(F_o)^2 + (0.095P)^2 + 0.29P]$, where $P = (F_o^2 + 2F_c^2)/3$, with the resulting $R = 0.059$, $R_w = 0.174$, and $S_w = 1.005$ (residual around solvent molecules $\Delta\rho < 0.38$ eÅ⁻³).

Results and Discussion

The synthesis of [Fe(TPC)(NH₂CH(CO₂CH₃)(CH(CH₃)₂))₂]CF₃SO₃ (**1**) is achieved by displacement of coordinate triflate from [Fe(TPC)]CF₃SO₃ according to the equation



Some difficulties are encountered in preparing amino ester ferric complexes of chlorins. First, the autoreduction of the ferric state can occur, as was previously reported with aliphatic amine ligands.^{40,41} Second, the binding constants of aliphatic amines to iron(III) porphyrins have been shown to be much smaller than those of the corresponding N-heterocycles.^{41–43} Thus, it is necessary to use a weak axial ligand such as triflate and an excess of ligand to prepare compound **1**. In solution, the complex has a green-black color and exhibits a visible spectrum with λ_{max} at 413, 548, 600, and 638 nm (CH₂Cl₂). Suitable crystals were obtained by diffusion of hexane in the dichloromethane solution of **1** in a thin tube.

Crystal Structure of [Fe(TPC)(NH₂CH(CO₂CH₃)(CH(CH₃)₂))₂]CF₃SO₃ (1**).** The molecule is a six-coordinate iron with four nitrogen atoms of the porphyrin and two nitrogen atoms of the axial ligands. An ORTEP diagram of the complex is shown in Figure 1, along with the atom numbering scheme. The most interesting bond distances and angles are summarized in Table 2.

Compound **1** has its amino ester ligands with the C–H α bonds directed toward two trans meso positions. Figure 1 also gives out-of-plane distances for the atoms in the chlorin core from the mean chlorin plane. The pyrrole and pyrroline atoms are only slightly displaced above and below the mean plane of the chlorin [maximum displacement of 0.04(2) Å]. Thus, the conformation of the chlorin macrocycle can be

(35) Otwinowski, Z.; Minor, W. *Methods Enzymol.* **1997**, *276*, 307–326.

(36) *International Tables for X-ray Crystallography*; Kluwer Academic Publishers: Dordrecht, The Netherlands, 1992; Vol. C.

(37) Spek, A. L. *PLATON. A Multipurpose Crystallographic Tool*; Utrecht University: Utrecht, The Netherlands, 1998.

(38) Altomare, A.; Burla, M. C.; Camalli, M.; Cascarano, G.; Giacovazzo, C.; Guagliardi, A.; Moliterni, A. G.; Polidori, G.; Spagna, R. *J. Appl. Crystallogr.* **1998**, *31*, 74–77.

(39) Sheldrick, G. M. *SHELXL97. Program for the Refinement of crystal Structures*; Göttingen University: Göttingen, Germany, 1997.

(40) Epstein, L. M.; Straub, D. K.; Maricondi, C. *Inorg. Chem.* **1967**, *6*, 1720–1724.

(41) Marsh, P. J.; Silver, J.; Symons, M. C. R.; Taiwo, F. A. *J. Chem. Soc., Dalton Trans.* **1996**, 2361–2369.

(42) Walker, F. A.; Simonis, U. *Encyclopedia of Inorganic Chemistry*; Wiley: Chichester: U.K., 1994; Vol. 4, pp 1785–1846.

(43) Beck, M. J.; Gopinath, E.; Bruce, T. C. *J. Am. Chem. Soc.* **1993**, *115*, 21–29.

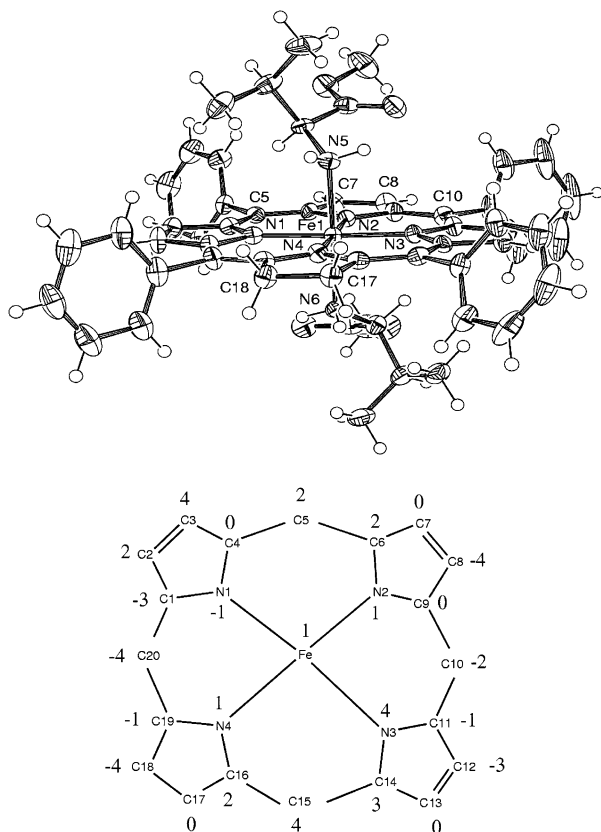


Figure 1. ORTEP diagram, atom labels, and formal diagram of the porphyrinato core showing deviations of each unique atom from the mean plane of the core (units of 0.01 ppm) for $[\text{Fe}^{\text{III}}(\text{TPC})(\text{Val-OMe})_2]\text{CF}_3\text{SO}_3$ (**1**).

Table 2. Selected Bond Distances (Å) and Angles (deg) for $[\text{Fe}^{\text{III}}(\text{TPC})(\text{Val-OMe})_2]\text{CF}_3\text{SO}_3$

bond	Å	bond	Å
Fe(1)–N(1)	1.996(4)	Fe(1)–N(6)	2.021(4)
Fe(1)–N(2)	2.012(4)	C(2)–C(3)	1.345(8)
Fe(1)–N(3)	1.984(4)	C(7)–C(8)	1.374(8)
Fe(1)–N(4)	2.034(4)	C(12)–C(13)	1.365(8)
Fe(1)–N(5)	2.039(4)	C(17)–C(18)	1.490(8)

angle	deg	angle	deg
N(1)–Fe(1)–N(3)	178.6(2)	N(3)–Fe(1)–N(5)	89.02(17)
N(1)–Fe(1)–N(5)	89.54(17)	N(3)–Fe(1)–N(6)	92.05(17)
N(1)–Fe(1)–N(6)	89.40(17)	N(4)–Fe(1)–N(5)	88.99(17)
N(2)–Fe(1)–N(4)	179.0(2)	N(4)–Fe(1)–N(6)	89.46(18)
N(2)–Fe(1)–N(5)	90.04(17)	N(5)–Fe(1)–N(6)	178.1(2)
N(2)–Fe(1)–N(6)	91.51(17)		

described as weakly distorted, indicating that the ground state is largely $(d_{xy})^2(d_{xz}d_{yz})^3$ (vide infra).

The C(17)–C(18) [1.490(8) Å] distance in the pyrroline ring is longer than the usual values of the three remaining pyrroles [average value of 1.361(8) Å] and reflects the sp^3 hybridization of the corresponding pyrroline carbon atoms. Such a situation was previously observed with three iron chlorins: the low-spin complex $[\text{Fe}(\text{TPC})(\text{PMe}_2\text{Ph})_2]\text{CF}_3\text{SO}_3$ [C–C distance = 1.446(16) Å],¹¹ the ferrous octaethylchlorin (OEC)Fe [C–C distance = 1.508(7) Å],²⁶ and with the μ -oxo complex $[(\text{TPC})\text{Fe}]_2\text{O}$ [C–C distance = 1.419(9) Å].²⁸

The metal–nitrogen distance to the reduced pyrrole N(4), 2.034(4) Å, is longer than the distances to nitrogen N(2) [2.012(4) Å] and to the two remaining nitrogens, N(1) and

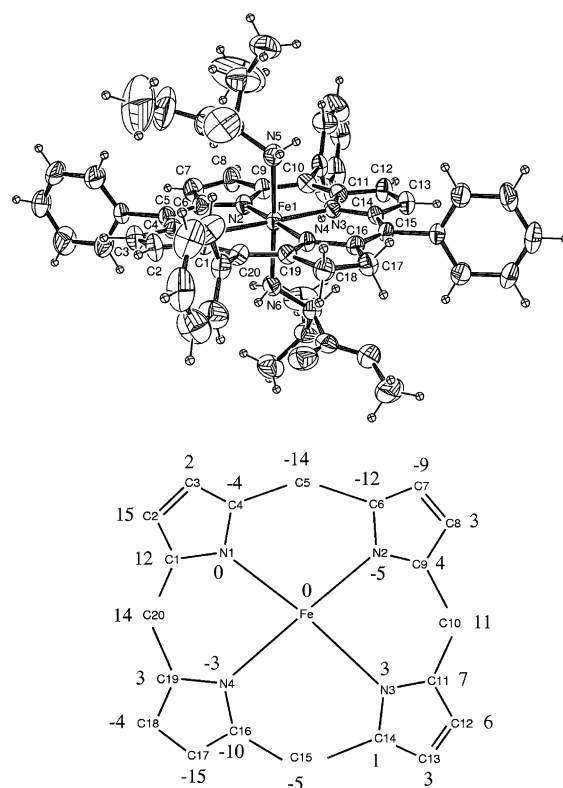


Figure 2. ORTEP diagram, atom labels, and formal diagram of the porphyrinato core showing deviations of each unique atom from the mean plane of the core (units of 0.01 ppm) for $[\text{Fe}^{\text{III}}(\text{TPC})(\text{Val-OMe})_2]$ (**2A**).

N(3) [average Fe–N distance = 1.990(4) Å]. These values are different from those found for low-spin ferric porphyrins such as $[\text{Fe}(\text{TPP})(1\text{-MeIm})_2]\text{ClO}_4$,⁴⁴ in which the four Fe–N distances average to 1.981(3) Å. Thus, there is a core–hole expansion of the macrocycle due to the reduced pyrrole. Such a situation, but to a lesser extent, was recently reported by us¹¹ in the comparison of the two complexes $[\text{Fe}(\text{TPC})(\text{PMe}_2\text{-Ph})_2]\text{CF}_3\text{SO}_3$ and $[\text{Fe}(\text{TPP})(\text{PMe}_2\text{Ph})_2]\text{CF}_3\text{SO}_3$.⁴⁵ The axial Fe–N(5) and Fe–N(6) distances are 2.039(4) and 2.021(4) Å, respectively. Thus, the average axial Fe–N(Val) distance of 2.030(4) Å is shorter than that in the analogue iron(II) complex of TPC containing the same ligand $[\text{Fe}(\text{TPP})(\text{L-Val})_2]$ [2.048(5) Å, see below].

Crystal Structure of $[\text{Fe}(\text{TPC})(\text{NH}_2\text{CH}(\text{CO}_2\text{CH}_3)(\text{CH}(\text{CH}_3)_2)_2]$ (2**).** The crystal structure of **2** comprises two independent molecules in the asymmetric unit of structure. The orientation of the ligands with respect to the porphyrin plane is not equivalent for the two independent molecules. The dihedral angle defined as C45–N56–Fe1–N4 is 138.3(2)° for **2A** and 58.7(2)° (C105–N65–Fe61–N64) for **2B**. The dihedral angle defined as C51–N6–Fe1–N4 is 67.8(2)° for **2A** and 38.1(2)° (C111–N66–Fe61–N64) for **2B**. The structures of **2A** and **2B** are shown in Figures 2 and 3, respectively. Individual values of bond distances and angles for **2A** and **2B** are reported in Table 3. Each molecule is a six-coordinate iron with four nitrogen atoms of the porphyrin and two nitrogen atoms of the axial ligands.

(44) Higgins, T. B.; Safo, M. K.; Scheidt, W. R. *Inorg. Chim. Acta* **1990**, *178*, 261–267.

(45) Simonneaux, G.; Sodano, P. *Inorg. Chem.* **1988**, *27*, 3956–3959.

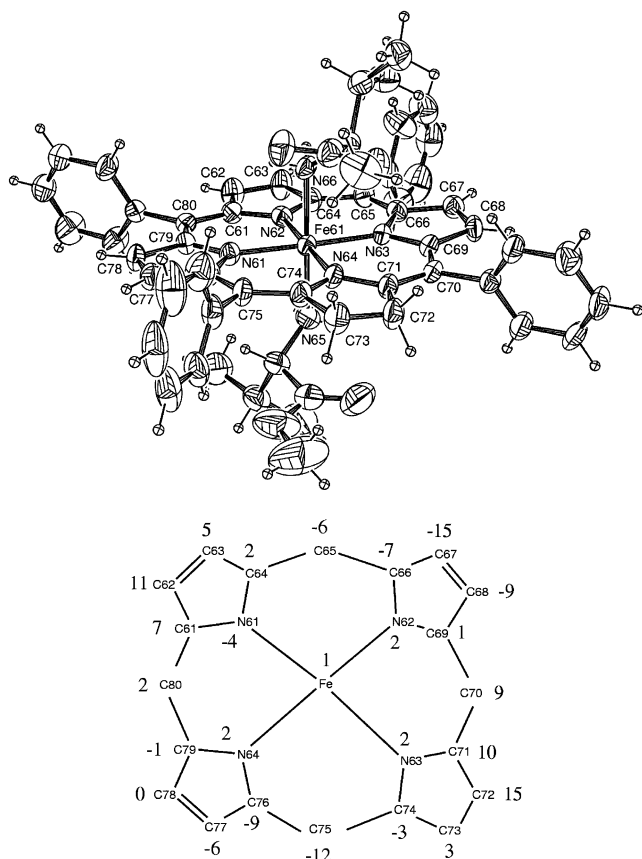


Figure 3. ORTEP diagram, atom labels, and formal diagram of the porphyrinato core showing deviations of each unique atom from the mean plane of the core (units of 0.01 ppm) for [Fe^{II}(TPC)(Val-OMe)₂] (**2B**).

Table 3. Selected Bond Distances (Å) and Angles (deg) for [Fe^{II}(TPC)(Val-OMe)₂] (**2**)

2A		2B	
bond	Å	bond	Å
Fe(1)–N(5)	2.038(6)	Fe(61)–N(65)	2.045(6)
Fe(1)–N(6)	2.059(6)	Fe(61)–N(66)	2.039(5)
Fe(1)–N(1)	1.988(5)	Fe(61)–N(61)	1.997(5)
Fe(1)–N(2)	2.005(6)	Fe(61)–N(62)	2.014(5)
Fe(1)–N(3)	2.015(5)	Fe(61)–N(63)	2.020(5)
Fe(1)–N(4)	1.991(5)	Fe(61)–N(64)	2.001(5)
C(2)–C(3)	1.382(11)	C(62)–C(63)	1.361(11)
C(7)–C(8)	1.372(11)	C(67)–C(68)	1.369(10)
C(12)–C(13)	1.334(11)	C(77)–C(78)	1.376(10)
C(17)–C(18)	1.411(10)	C(72)–C(73)	1.407(10)
angle	deg	angle	deg
N(5)–Fe(1)–N(6)	177.3(2)	N(65)–Fe(61)–N(66)	174.7(3)
N(3)–Fe(1)–N(1)	178.8(2)	N(61)–Fe(61)–N(64)	90.7(2)
N(3)–Fe(1)–N(4)	89.7(2)	N(63)–Fe(61)–N(64)	90.3(2)
N(1)–Fe(1)–N(4)	91.4(2)	N(61)–Fe(61)–N(62)	89.7(2)
N(3)–Fe(1)–N(2)	89.3(2)	N(63)–Fe(61)–N(62)	89.4(2)
N(1)–Fe(1)–N(2)	89.7(2)	N(64)–Fe(61)–N(62)	179.4(2)
N(4)–Fe(1)–N(2)	177.0(2)	N(61)–Fe(61)–N(66)	89.7(2)
N(3)–Fe(1)–N(6)	93.7(2)	N(63)–Fe(61)–N(66)	89.1(2)
N(1)–Fe(1)–N(6)	87.0(2)	N(64)–Fe(61)–N(66)	92.8(2)
N(4)–Fe(1)–N(6)	89.5(2)	N(62)–Fe(61)–N(66)	87.7(2)
N(2)–Fe(1)–N(6)	87.7(2)	N(61)–Fe(61)–N(65)	92.5(2)
N(3)–Fe(1)–N(5)	88.4(2)	N(63)–Fe(61)–N(65)	88.7(2)
N(1)–Fe(1)–N(5)	90.9(2)	N(64)–Fe(61)–N(65)	92.0(3)
N(4)–Fe(1)–N(5)	92.2(2)	N(62)–Fe(61)–N(65)	87.5(3)
N(2)–Fe(1)–N(5)	90.6(2)	N(61)–Fe(61)–N(63)	178.4(2)

The metal–nitrogen distances to the reduced pyrrole N(4), 1.991(5) Å, and to the pyrrole trans to it N(2), 2.005(6) Å,

are slightly different from the distances to the two remaining nitrogens, N(1), 1.988(5) Å, and N(3), 2.015(5) Å [average Fe–N distance = 2.000(5) Å], in **2A**. A similar situation was found in **2B**: Fe–N(64) = 2.001(5) Å, and average Fe–N distance = 2.008(9) Å. In [Fe(TPP)(1-BuNH₂)₂], [Fe(TPP)(PhCH₂NH₂)₂], and [Fe(TPP)(PhCH₂CH₂NH₂)₂], the Fe–N distances average 1.987(2), 1.992(2), and 1.989(2) Å, respectively.⁴⁶ This is in agreement with the values for other low-spin iron(II) porphyrin structures [range = 1.970(14)–2.000(6) Å].⁴⁷ Thus, there is a core–hole expansion of the macrocycle due to the reduced pyrrole. Such a situation has been previously reported for high-spin iron(III) quinoxalino-tetraphenylporphyrin²¹ and discussed in terms of molecular mechanics calculations.^{48,49}

The C(17)–C(18) [**2A**, 1.411(10) Å; **2B**, 1.407(10) Å] distance in the pyrroline ring is longer than the usual values of the three remaining pyrroles [average value of 1.362(10) Å] and reflects the sp³ hybridization of the corresponding pyrroline atoms. Such a situation was previously observed with two iron chlorins: the ferrous octaethylchlorin (OEC)-Fe [C–C distance = 1.508(7) Å]²⁶ and the μ -oxo complex [(TPC)Fe]₂O [C–C distance = 1.419(9) Å].²⁸

The pyrrole and pyrroline rings are only slightly displaced above and below the mean plane of the chlorin [maximum displacement = 0.15(2) Å for **2A** and 0.15(2) Å for **2B**]. Thus, the conformation of the chlorin macrocycle can be described as weakly distorted. Figures 2 and 3 also give out-of-plane distances for the atoms in the chlorin core from the mean chlorin plane.

The axial Fe–N distances, Fe(1)–N(5) and Fe(1)–N(6) (2.038 and 2.059 Å, respectively), in **2A** are only slightly longer than the corresponding distances in the iron(III) complex **1** of TPC containing the same ligand [2.030(4) Å]. This might reflect the facts that iron(II) has a slightly larger radius than iron(III) and that **1** is slightly ruffled. The axial Fe–N distances of **2** are very similar to those in the iron(II) complexes of tetraphenylporphyrin containing primary amines, reported by Munro et al.⁴⁶ for [Fe(TPP)(1-BuNH₂)₂], [Fe(TPP)(PhCH₂NH₂)₂] and [Fe(TPP)(PhCH₂CH₂NH₂)₂] as 2.390(3), 2.0435(3), and 2.028(2) Å, respectively. In the crystal structure of cytochrome *f*, the tyrosine-1 amino N–Fe bond distance is 2.0 Å, in agreement with our results. However, the protein structure is refined to 2.3 and then 1.96 Å,^{29,30} and a more precise comparison is not possible.

¹H NMR Spectroscopy. The ¹H NMR spectrum of [Fe(TPC)(NH₂CH(CO₂CH₃)(CH(CH₃)₂))₂]CF₃SO₃ (**1**) at 298 K is shown in Figure 4. The peaks for the phenyl protons of the chlorin ring are assigned by 2D COSY spectra. For the axial ligands and the pyrroles, the relative intensities and a comparison with the analogue porphyrin complex³³ determine the assignments. Although the resonance intensities are large, the shifts of the valine ester ligands are independent of the

(46) Munro, O. Q.; Madlala, P. S.; Warby, R. A. F.; Seda, T. B.; Hearne, G. *Inorg. Chem.* **1999**, *38*, 4724–4736.

(47) Scheidt, W. R.; Reed, C. A. *Chem. Rev.* **1981**, *81*, 543–555.

(48) Eschenmoser, A. *Ann. N.Y. Acad. Sci.* **1986**, *471*, 108.

(49) Kaplan, W. A.; Suslick, K. S.; Scott, R. A. *J. Am. Chem. Soc.* **1991**, *113*, 9824–9827.

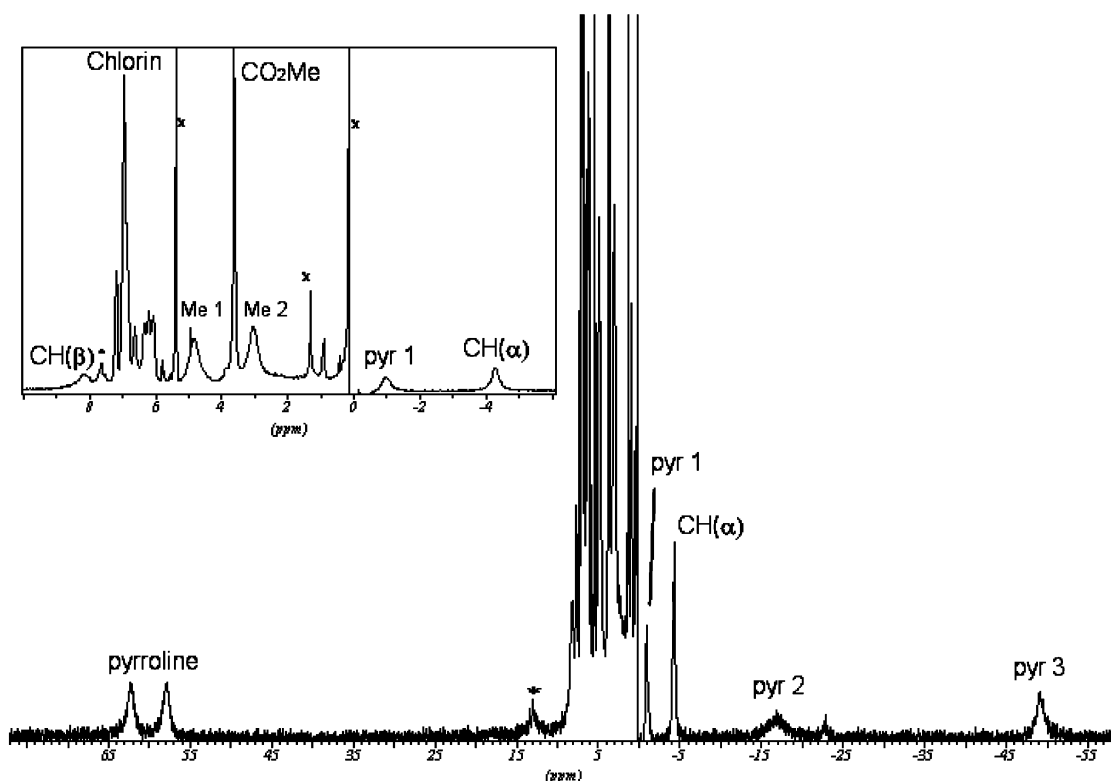


Figure 4. ^1H NMR spectrum of $[\text{Fe}(\text{TPC})(\text{Val-OMe})_2]\text{CF}_3\text{SO}_3$ (**1**) recorded at 283 K in CD_2Cl_2 . * = *m*-oxo complex.

Table 4. Observed and Isotopic Shifts of $[\text{Fe}(\text{TPC})(\text{NH}_2\text{CH}(\text{CO}_2\text{CH}_3)(\text{CH}(\text{CH}_3)_2)_2]\text{CF}_3\text{SO}_3$ (**1**) 298 K (δ , CD_2Cl_2 , ppm)

chlorin												
proton	Ho	Ho'	Hm	Hm'	Hp	Hp'	Hpyrro1	Hpyrro2	Hpyr	Hpyr	Hpyr	Hpyr
$(\Delta H/H)^a$	6.09	6.43	6.8	6.84	7.12	6.77	57.3	61.26	-0.8	-16.45	-48.33	
$(\Delta H/H)^b$	7.6	7.8	7.6	7.6	7.6	7.6	4.35	4.35	7.6	8.2	7.6	
$(\Delta H/H)^c$	-1.5	-1.4	-0.8	-0.76	-0.48	-0.83	52.95	56.91	-8.4	-24.65	-55.93	
ligand												
Val-OMe	CH(α)	CH(β)	CH ₃ ¹	CH ₃ ²	CO ₂ Me	NH ₂						
$(\Delta H/H)^a$	-4.18	8.03	4.66	2.94	3.53	175.6						
$(\Delta H/H)^d$	-2.44	-0.5	-0.78	-1.06	2.41	-6.52, -5.06						
$(\Delta H/H)^e$	-1.74	8.53	5.44	4	1.12	181.4						

^a Chemical shift of $[\text{Fe}(\text{TPC})(\text{NH}_2\text{CH}(\text{CO}_2\text{CH}_3)(\text{CH}(\text{CH}_3)_2)_2]\text{CF}_3\text{SO}_3$ (**1**) at 298 K with TMS as an internal reference. ^b Chemical shift of $[\text{Fe}(\text{TPC})(\text{PMe}_2\text{Ph})_2]$ at 298 K with TMS as an internal reference.¹¹ ^c Isotopic shift of **1** with diamagnetic complex $[\text{Fe}(\text{TPC})(\text{PMe}_2\text{Ph})_2]$ as the reference.¹¹ We used a medium value of 7.8 ppm for the chemical shifts of the diamagnetic pyrroles because the relative assignment was not possible at this stage ^d Chemical shift of the amino ester ligand complexed to a diamagnetic ruthenium porphyrin complex at 298 K with TMS as an internal reference.⁵³ ^e Isotopic shift of **1** with a diamagnetic bis($\text{NH}_2\text{CH}(\text{CO}_2\text{CH}_3)(\text{CH}(\text{CH}_3)_2)$) Ru(II) complex as the reference.⁵³

presence of excess ligand. Hence, axial ligand exchange is slow on the NMR time scale, as judged by the presence of both coordinated and free signals at ambient temperature. Magnetic measurements using the method of Evans^{50,51} were made for 0.03 M CD_2Cl_2 solutions of **1** at 298 K, employing Me_4Si as the reference. The solution magnetic moment ($\mu = 1.91 \mu_{\text{B}}$) is compatible with a low-spin state, $S = 1/2$. The hyperfine shifts, obtained by referencing the observed shift to that of the corresponding diamagnetic complex $\text{Fe}(\text{TPC})\text{-}(\text{PPh}(\text{Me})_2)_2$,¹¹ are summarized in Table 4.

The hyperfine shifts for symmetrical low-spin ferric porphyrins are known to consist of large contact shifts and smaller upfield dipolar shifts due to the magnetic anisotropy.

In chlorin, the symmetry is lost, but La Mar and co-workers have suggested that such a situation is also highly probable with low-spin ferric chlorins.¹⁶

Pyrrole. The spectrum of **1** shows the pyrrole proton signals at -0.8, -16.4, and -48.3 ppm (298 K). This is quite different from the pyrrole proton signals of two other low-spin iron(III) chlorinates at ambient temperature, namely, $[\text{Fe}(\text{TPC})(\text{PMe}_2\text{Ph})_2]\text{CF}_3\text{SO}_3$ (0.66, 0.66, and -57.8 ppm)¹¹ and $[\text{Fe}(\text{QTPP})(\text{Im})_2]^+$ (-12.2, -15.6, and -21.7 ppm, 293 K),²¹ but close to the pyrrole proton signals of $[\text{Fe}(\text{TMC})\text{-}(\text{Im})_2]\text{Cl}$ (-2.4, -12.3, and -47.1 ppm, 203 K).¹⁹

Pyrroline. For the saturated pyrroline ring, the protons are expected to exhibit low-field π -contact shifts.¹⁶ The CH_2 groups of the reduced pyrroles appear as two signals at 298 K (57.3 and 61.3 ppm). It should be noted that the ligands

(50) Evans, D. F. *J. Chem. Soc.* **1959**, 2003–2005.

(51) Sur, S. K. *J. Magn. Res.* **1989**, 82, 169–173.

are optically active and the nonequivalence might be due to a diastereoisomerism. These observed large low-field shifts for **1** agree with an important π metal bonding scheme involving a molecular orbital of the chlorine derived either from the a_{1u} orbital¹⁰ or from the $3e$ π -orbital of a porphyrin.²² This contact shift is very similar to that of the corresponding [Fe(TPC)(PPh(Me)₂)₂]CF₃SO₃ ($\delta = 69$ ppm)¹¹ and [Fe-(TMC)(Im)₂]Cl ($\delta = 38.3$ ppm)¹⁹ complexes and not too far from those of pyropheophorbide, a methylester iron(III) ($\delta = 24$ and 28 ppm).¹⁶ Because the contact shift has been shown to arise predominantly from spin delocalization into the bonding d_{xz} and d_{yz} orbitals,¹⁶ the results agree with a $(d_{xy})^2(d_{xz}, d_{yz})^3$ electronic structure in this amino ester derivative (see below).

Phenyl. In contrast to the pyrrole protons, the phenyl protons exhibit weak isotropic shifts that were found to be essentially dipolar in origin (Table 4). Thus, a plot $(\Delta H/H)$ -iso vs $(3 \cos^2 \theta - 1)/r^3$ for all protons is linear and confirms the quasi absence of contact shift in this position (not shown).

Ligand. A broad resonance for the coordinated NH₂ group is detected at 175.6 ppm for **1**. This peak is assigned on the basis of the chemical shift of coordinated ammonia (240.6 ppm) in bis(ammonia)-ligated low-spin iron(III) porphyrin derivative⁵² and coordinated L-valine ester (265 ppm) in [Fe-(TPP)(L-Val)₂]CF₃SO₃.³³ The shift of the NH₂ is at low field because of the σ -delocalization at that position. In comparison with the analogue complex with porphyrin, the effects are similar but with a much lesser extent in the chlorine case ($\Delta\delta = 90$ ppm). This decrease is probably due to a larger contribution of iron chlorine than iron porphyrin to the σ -donation to iron.

Because saturation transfer experiments were not possible with the chlorine complex, we used chemical shifts of the protons of the L-valine ester ligands of [Fe(PPP)(L-Val)₂]-CF₃SO₃ as a reference for the assignment.³³ The hyperfine shifts, obtained by referencing the observed shift to that of a corresponding diamagnetic bis(valine methyl ester) ruthenium(II) complex,⁵³ are summarized in Table 4. The ¹H NMR spectrum for **1** also exhibited the expected separate resonances for each of the diastereotopic methyl group of the ligand. The difference is much larger for the complex than for the free ligand.

Analysis of the curve in the Curie plot was made for the [Fe(TPC)(NH₂CH(CO₂CH₃)(CH(CH₃)₂)₂)CF₃SO₃ complex. The temperature dependences of the chemical shifts of the protons in CD₂Cl₂ are shown in Figure 5. A magnetically simple molecule is expected to follow Curie-law behavior in that a plot of the chemical shifts vs $1/T$ is linear with an intercept equal to the resonance in the diamagnetic complex. Plots of ortho, meta, and para signals of meso-aryl protons of the chlorine ring are reasonably linear and have intercepts of 8.03, 7.4, and 7.34 ppm, respectively. However, these protons show only small temperature dependences, consistent with a weak spin density at the meso position. For the pyrrole

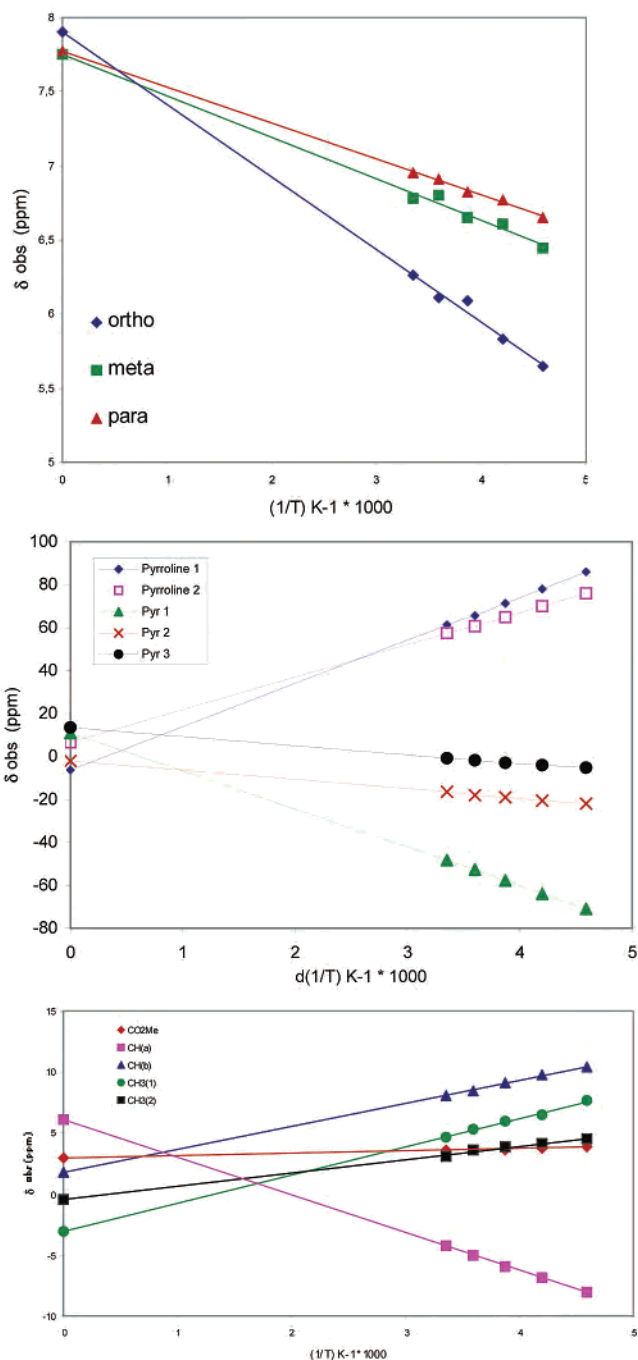


Figure 5. Curie plots of the isotropic shifts versus reciprocal temperature of [Fe(TPC)(Val-OMe)₂]CF₃SO₃ (**1**) in CD₂Cl₂.

resonances, the chemical shifts vary linearly with $1/T$, but the extrapolated lines do not pass through the diamagnetic value at $1/T = 0$ (Figure 5). We were not able to record the ¹H NMR spectrum of [Fe(TPC)(NH₂CH(CO₂CH₃)(CH(CH₃)₂)₂)] because of its rapid decomposition in solution to give unidentified paramagnetic species.

EPR Spectroscopy. Among the heme proteins, the paramagnetic states of iron are particularly amenable to spectroscopic investigations by electron paramagnetic resonance (EPR).⁵⁴ Thus, EPR spectroscopy has been used for

(52) Oh, Kim, Y.; Goff, H. M. *Inorg. Chem.* **1990**, *29*, 3907.

(53) Morice, C.; Le Maux, P.; Moinet, C.; Simonneaux, G. *Inorg. Chim. Acta* **1998**, *273*, 142–150.

(54) Peisach, J.; Blumberg, W. E.; Adler, A. D. *Ann. N.Y. Acad. Sci.* **1973**, *206*, 310–327.

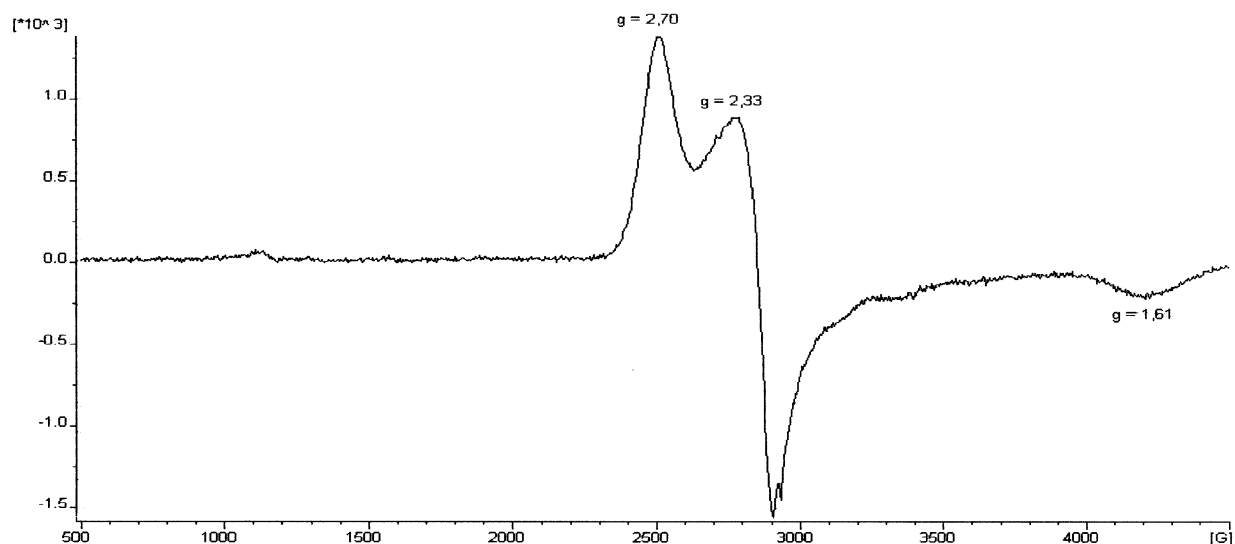


Figure 6. EPR spectrum of $[\text{Fe}(\text{TPC})(\text{Val-OMe})_2]\text{CF}_3\text{SO}_3$ (**1**) in a CH_2Cl_2 glass, recorded at 4 K.

classifying low-spin ferriheme proteins and model porphyrin complexes on the basis of a crystal field analysis developed by Griffith.⁵⁵ Continuous-wave EPR yields only the absolute values of the components of the g tensors and not their orientation with respect to the molecular frame. Because it was found recently²² that the orientation and electronic ground states are not necessarily those expected on the basis of the Taylor analysis,⁵⁶ which assumes that the rhombicity must be less than $2/3$, our proposition cannot be considered definitive. However, our EPR results, strongly suggest a $(d_{xy})^2(d_{xz}, d_{yz})^3$ ground state. Thus, the EPR spectrum of CH_2Cl_2 frozen solutions of complex **1** shows rhombic EPR signals with $g_1 = 2.70$, $g_2 = 2.33$, and $g_3 = 1.61$ ($\Sigma g^2 = 15.3$) (Figure 6). The principal g values for the similar complexes $[\text{Fe}(\text{TPC})(\text{PPh}(\text{Me})_2)_2]\text{CF}_3\text{SO}_3$ and $[\text{Fe}(\text{TPC})(\text{Im})_2]\text{Cl}$ are $g_1 = 2.51$, $g_2 = 2.37$, and $g_3 = 1.74$ ($\Sigma g^2 = 14.9$)¹¹ and $g_1 = 2.49$, $g_2 = 2.39$, and $g_3 = 1.75$ ($\Sigma g^2 = 15.0$),²² respectively. In contrast, for $[\text{Fe}(\text{TPC})(\text{CN-}t\text{-Bu})_2]\text{CF}_3\text{SO}_3$, where $\Sigma g^2 = 13.1$ is much lower, a considerable amount of orbital angular momentum is quenched in this complex according to a $(d_{xz}, d_{yz})^4(d_{xy})^1$ ground state.¹² This interpretation is also supported by a recent EPR results on $[\text{Fe}(\text{TPC})(\text{Im})_2]\text{Cl}$ reported by Walker et al. showing that the highest g value is g_z .²²

Conclusion

In conclusion, these spectroscopic observations are indicative of a metal-based electron in the d_π orbitals for the $[\text{Fe}(\text{TPC})(\text{NH}_2\text{CH}(\text{CO}_2\text{CH}_3)(\text{CH}(\text{CH}_3)_2)_2)]\text{CF}_3\text{SO}_3$ complex at

any temperature. Thus, the change in ground state of low-spin Fe(III) from the usual $(d_{xy})^2(d_{xz}, d_{yz})^3$ to the unusual $(d_{xz}, d_{yz})^4(d_{xy})^1$ electron configuration, which was previously suggested to occur from porphyrin to chlorin macrocycles,⁵⁴ is not observed with amino ester ligands. However, the unusual $(d_{xz}, d_{yz})^4(d_{xy})^1$ electron configuration of low-spin Fe(III) is possible both with porphyrin and chlorin macrocycles but seems largely related to the π -acceptor properties⁵⁷ of the ligands such as isocyanide^{12,58–61} and phosphonite.⁶²

Supporting Information Available: CIF data for bis(L-valine methyl ester)(*meso*-tetraphenylchlorin)iron(III)triflate and bis(L-valine methyl ester)(*meso*-tetraphenylchlorin)iron(II). This material is available free of charge via the Internet at <http://pubs.acs.org>.

IC026039H

- (55) Griffith, J. S. *Nature* **1957**, *180*, 30–31.
 (56) Taylor, C. P. S. *Biochim. Biophys. Acta* **1977**, *491*, 137–149.
 (57) Ghosh, A.; Gonzales, E.; Vangberg, T. *J. Phys. Chem. B* **1999**, *103*, 1363–1367.
 (58) Simonneaux, G.; Bondon, A. *The Porphyrin Handbook*; Kadish, K. M., Smith, K. M., Guillard, R., Eds.; Academic press: New York, 2000; Vol. 5, Chapter 38, pp 299–322.
 (59) Simonneaux, G.; Schünemann, V.; Morice, C.; Carel, L.; Toupet, L.; Winkler, H.; Trautwein, A. X.; Walker, F. A. *J. Am. Chem. Soc.* **2000**, *122*, 4366–4377.
 (60) Walker, F. A.; Nasri, H.; Turowska-Tyrk, I.; Mohanrao, K.; Watson, C. T.; Shokhirev, N. V.; Debrunner, P. G.; Scheidt, W. R. *J. Am. Chem. Soc.* **1996**, *118*, 12109–12118.
 (61) Simonneaux, G.; Hindré, F.; Le Plouzenec, M. *Inorg. Chem.* **1989**, *28*, 823–825.
 (62) Pilard, M. A.; Guillemot, M.; Toupet, L.; Jordanov, J.; Simonneaux, G. *Inorg. Chem.* **1997**, *36*, 6307–6314.